LA-9498-MS

UC-33
Issued: September 1982

Nuclear Reactor System Study for NASA/JPL

Final Report

R. G. Palmer
L. B. Lundberg
E. S. Keddy
D. R. Koenig

Los Alamos National Laboratory
Los Alamos, New Mexico 87545

NUCLEAR REACTOR SYSTEM STUDY FOR NASA/JPL
FINAL REPORT

by

R. G. Palmer, L. B. Lundberg, E. S. Keddy, and D. R. Koenig

ABSTRACT

Reactor shielding and safety studies and heat pipe development work undertaken for the Jet Propulsion Laboratory during the period March 1, 1981 to October 30, 1981 are described. Monte Carlo caluclations of gamma and neutron shield configurations show that substantial weight penalties are incurred if exposures at 25 m to neutrons and gammas must be limited to 10^{12} nvt and 10^{6} rad, instead of the 10^{13} nvt and 10^{7} rad values used earlier. For a 1.6 MW_t reactor, the required shield weight increases from 400 to 815 kg.

Water immersion criticality calculations have been extended to study the effect of water in fuel void spaces as well as in the core heat pipes. These show that the insertion into the core of eight blades of B_4C with a mass totaling 2.5 kg will guarantee subcriticality.

The design, fabrication procedure, and testing of a 4-in-long molybdenum/lithium heat pipe are described. It appears that an excess of oxygen in the wick prevented the attainment of expected performance capability.

I. INTRODUCTION

As part of a program to develop technology for application to nuclear electric systems capable of propelling large payloads on orbital missions to the outer planets, the National Aeronautics and Space Administration (NASA), through the Jet Propulsion Laboratory (JPL), has supported work at Los Alamos National Laboratory on space nuclear reactor design and component development. The work

has been directed primarily towards those aspects of space reactor design that are most influenced by the propulsion application. Specifically, this includes work on shield design, safety studies, and the design and testing of long heat pipes for coupling reactor core heat to a heat conversion system. Reactor shielding for the nuclear electric propulsion mission is a more difficult problem than for orbital power supplies, mostly because experimenters concerned with the science payload are anxious to keep radiation background to a minimum. Thus, the tolerable exposures at 25 m from the reactor have been reduced to 10^{12} nvt and 10^{6} rad, rather than the values of 10^{13} nvt and 10^{7} rad used for orbital application.

The safety investigation concerned methods of guaranteeing subcriticality of the reactor heat source even when it is immersed in water. These studies are applicable to heat pipe reactor sources in general, rather than being directed toward a specific application.

The work on developing very long (4 m) heat pipes, while initiated to prove out a specific thermionic reactor design, has been pursued most recently because of the NASA interest in developing heat pipe reactor systems that are radiatively coupled to thermoelectric conversion systems.

II. SPACE REACTOR SHIELDING STUDIES

The reactor shielding studies consisted of a series of calculations that was performed to ascertain shielding requirements for a heat pipe reactor system as a function of reactor power. The power was varied from 0.6 MW_t to 2.0 MW_t, and two sets of constraints were used for acceptable radiation doses at the payload (25 m from the reactor), namely, 10^{12} nvt neutrons/10^{6} rad gammas and 10^{13} nvt neutrons/10^{7} rad gammas. The shield half-angle was maintained at 15°.

The Los Alamos MCNP Monte Carlo code was used in several stages. K_{eff} calculations were made for each reactor power to determine the magnitudes and spectra of the neutrons and gammas leaking from the reactor. Over the range of power levels examined, the leakage spectra were similar within the statistics of the MCNP tallies, and the magnitudes of the leakages were such as to justify a linear relationship between magnitude and power. The calculated neutron and

gamma leakage spectra are listed in Table I. These calculated leakages were used as the source of neutron and gamma radiation in the shielding calculations. The source was uniformly distributed in the volume that would be occupied by the reactor, but the reactor materials were not included in the calculations.

Two types of shielding calculations were performed. Some of the neutrons leaving the reactor produce gammas by absorption and inelastic scattering in the shield and in thermoelectric and radiator components between the reactor and the payload. Thus the MCNP code was used in the dual neutron-gamma mode to predict the neutron fluence and the gamma dose resulting from neutron interactions external to the reactor. This gamma dose was added to that calculated by MCNP in the gamma mode, based on the fates of the gammas leaving the reactor.

The reactor-shield configuration is shown in Fig. 1. The four design parameters θ, ψ, ω, and L are shown in the figure. Previous shielding studies indicated an asymptote of dose vs decreasing ψ. To avoid problems arising from interference by the overlapping shield with cooling of the control rods and radial reflector surfaces by radiation heat transfer, the optimum value of ψ was chosen to be 30°. The next step was to determine the optimum value of ω for a given value of L. A separate study showed that the minimum dose rate for a given shield weight occurs when the value of ω is such that the ratio of the length of the conical outside surface of the shield, L_s, to the centerline thickness, L, is about 0.95. This behavior is shown for two shield masses, 400 kg and 700 kg, in Figs. 2 and 3, respectively.

The shield design was assumed to be a tungsten-face gamma shield several centimeters thick, followed by a LiH neutron shield (plus stainless steel structure) between 65 and 90 cm thick. For a 1.2 MW_t reactor power the neutron fluence vs mass of LiH + SS is shown in Fig. 4. Figure 5 shows the effect of adding a tungsten gamma shield on the dose rate at the payload.

The results of the study are shown in Table II, which gives the required neutron and gamma shield masses for two sets of dose criteria.

III. WATER IMMERSION CRITICALITY STUDIES

Previous calculations of the quantity of boron carbide required to compensate for the reactivity effects of water immersion of a 1.2-MW_t heat pipe

TABLE I

LEAKAGE SPECTRUM FROM 1.2-MW_t REACTOR

Neutrons		Gammas	
E_N	Percent	E_N	Percent
17 MeV	0	7 MeV	0.01
15	0	6	0.56
13.5	0	5	1.44
12.0	0.04	4	3.63
10	0.23	3	1.50
7.79	0.46	2.5	1.98
6.07	2.63	2.0	4.66
3.68	3.89	1.5	10.51
2.232	4.60	1.0	4.74
1.738	5.17	0.8	4.69
1.353	7.32	0.7	3.89
823 keV	5.78	0.6	4.96
500	6.13	0.5	10.75
303	5.60	0.4	7.19
184	9.03	0.3	9.04
67.6	8.10	0.2	13.57
24.8	6.98	0.1	11.02
9.12	6.34	0.05	4.52
3.35	5.43	0.03	1.12
1.235	4.47	0.01	0.19
454 eV	3.41	0.005	0.04
167	3.01		
61.4	2.23		
22.6	1.82		
8.32	1.40		
3.06	1.21		
1.13	1.03		
0.414	3.69		

1.2 MW_t = 7.05×10^{16} γ/s

1.2 MW_t = 3.18×10^{16} n/s

TABLE II

NEUTRON, GAMMA, AND TOTAL SHIELD WEIGHTS FOR VARIOUS REACTOR POWERS AND PAYLOAD RADIATION LIMITATIONS

	10^{12} nvt/10^{6} rad			10^{13} nvt/10^{7} rad		
P MW	LiH + SS kg	W kg	Total kg	LiH + SS kg	W kg	Total kg
0.6	370	175	545	225	0	225
0.8	400	215	615	265	0	265
1.0	432	250	682	300	0	300
1.2	455	275	730	325	0	325
1.4	475	300	775	345	20	365
1.6	495	320	815	360	40	400
1.8	5[illegible]	335	850	370	60	430
2.0	533	350	883	380	85	465

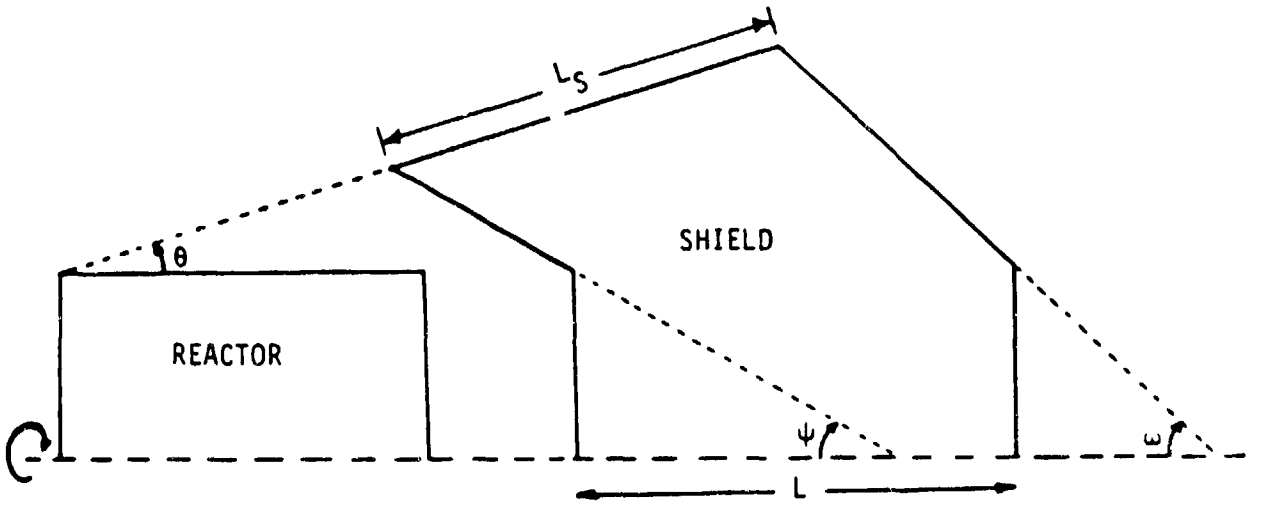

Fig. 1. Reactor-shield configuration.

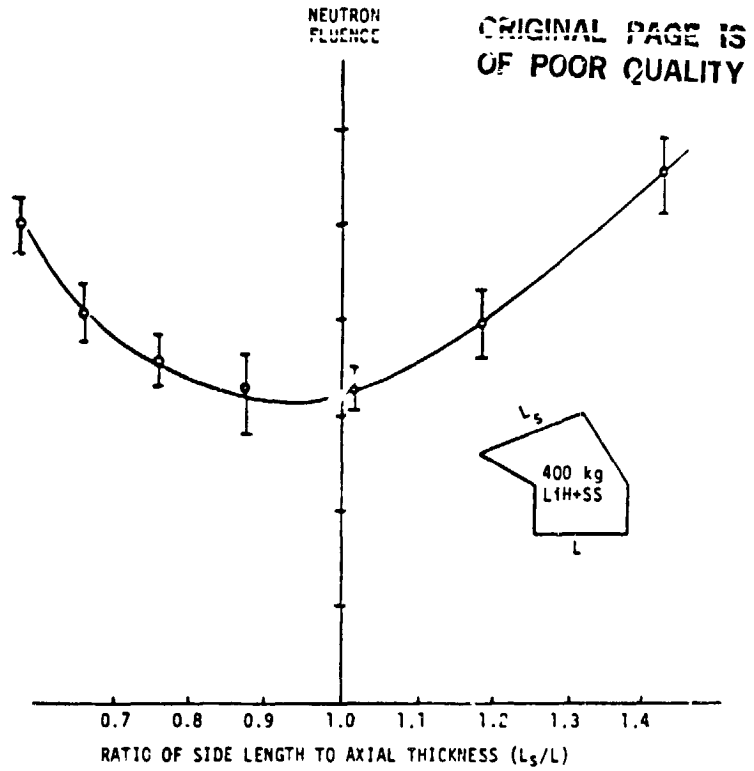

Fig. 2. Effect of ratio of shield side length to central thickness on shielding effectiveness for a constant shield mass of 400 kg.

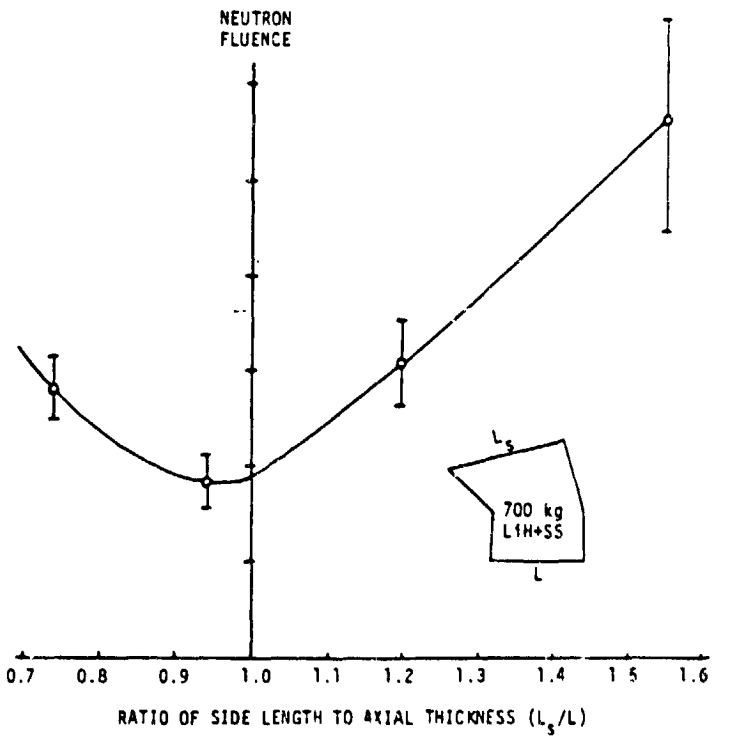

Fig. 3. Effect of ratio of shield side length to central thickness on shielding effectiveness for a constant shield mass of 700 kg.

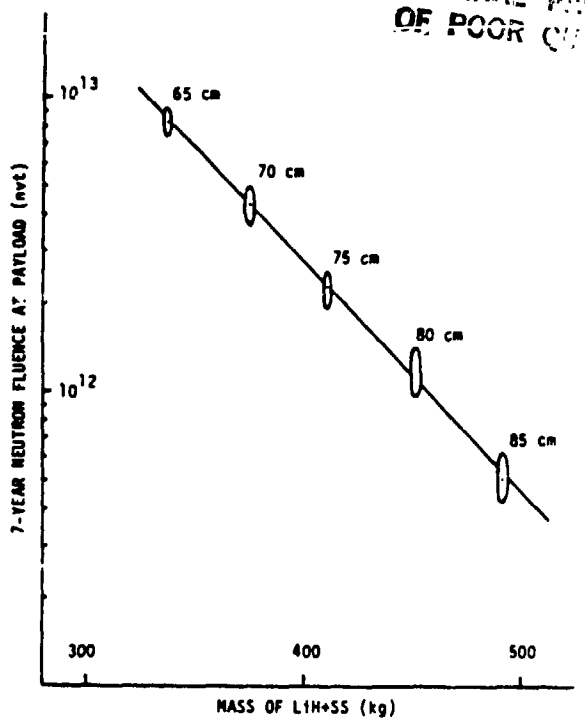

Fig. 4. Neutron fluence as a function of shielding mass for a reactor power of 1.2 MW_t. The numbers associated with each data point represent the shield thickness.

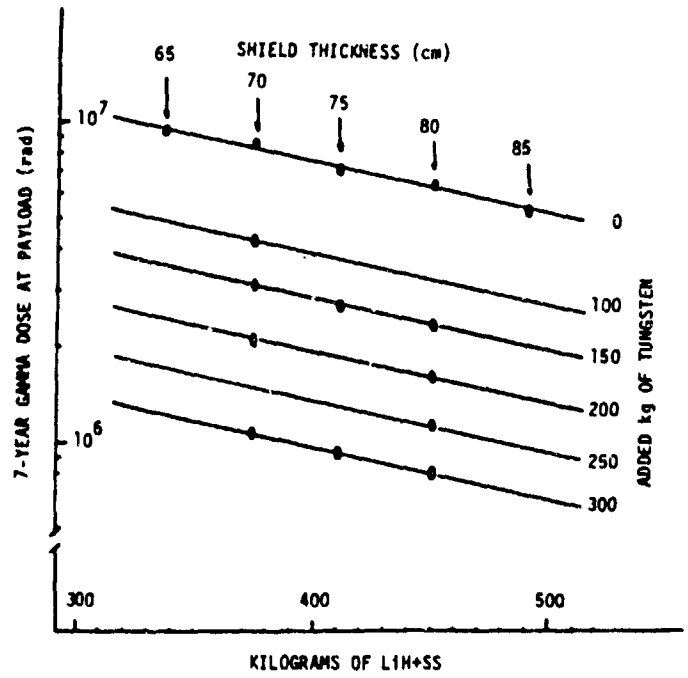

Fig. 5. Effect of added tungsten gamma shield on dose rate at payload.

reactor in a lake or the ocean assumed, for computational expediency, that the B_4C could be placed in twelve of the core heat pipes. More practical arrangements were studied in which radial slots in the fuel between core heat pipes (see Fig. 6) are occupied by enriched B_4C until a safe orbit is achieved, at which time the B_4C will be displaced by molybdenum.

The previous calculations considered only water entering the core heat pipes and not the spaces between fuel tiles, which allow some fuel swelling with burnup. The effects of water entering both the heat pipes and the swelling spaces have now been calculated. The results for various dry and flooded configurations and with B_4C and molybdenum in the radial slots are shown in Table III. The total amount of enriched B_4C in the eight core slots is 2.5 kg.

It can be seen from Table III that the additional effect of water entering the swelling spaces is also a positive reactivity. With the control drum (50% enriched ^{10}B in B_4C) in the shutdown position, the effect of flooding renders the core just short of criticality when B_4C is in the slots and highly supercritical with molybdenum in the slots.

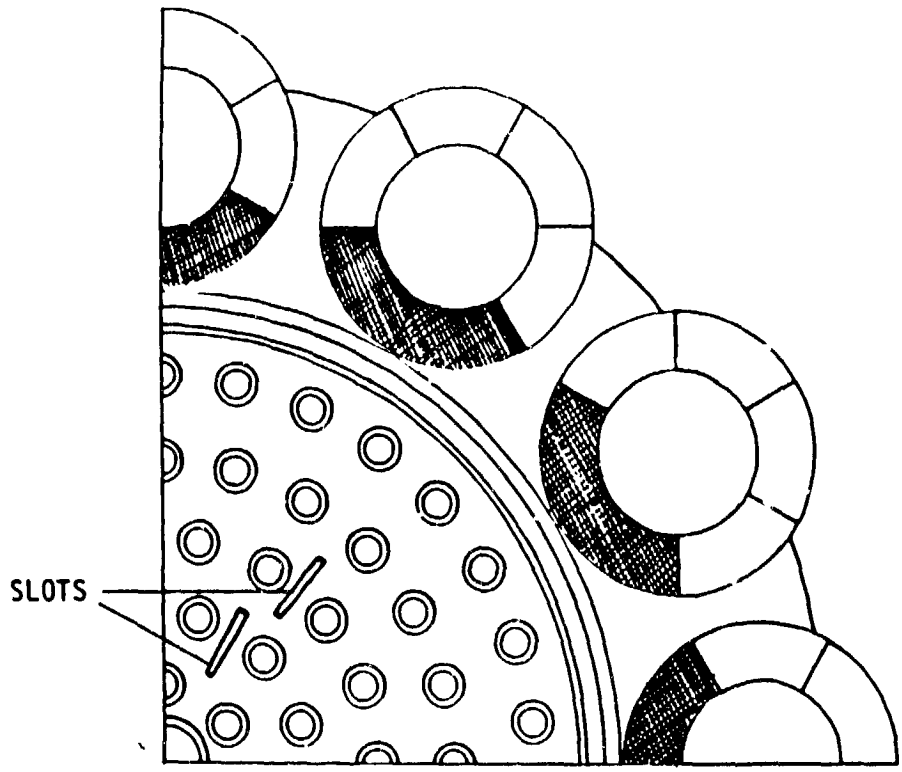

Fig. 6. Diagram showing radial slots in fuel between core heat pipes.

TABLE III

CALCULATED MULTIPLICATION FACTOR k_{eff} FOR
VARIOUS DRY AND FLOODED CONFIGURATIONS

	Dry	Heat Pipes Flooded	Heat Pipes and Void Flooded	
90% enriched control drums	0.912 ± 0.004	1.080 ± 0.003	1.104 ± 0.003	Mo in slots
	0.812 ± 0.004	0.924 ± 0.003	0.950 ± 0.003	B_4C in slots
50% enriched control drums	0.935 ± 0.005	1.096 ± 0.004	1.122 ± 0.004	Mo in slots
	0.891 ± 0.004	1.010 ± 0.003	0.998 ± 0.002	B_4C in slots

Future studies will investigate the possibility of employing a single, centrally located, B_4C plug to achieve the same effect as the slots.

IV. FABRICATION AND TESTING OF 4-M MOLYBDENUM/LITHIUM HEAT PIPE

A. Design.

The 4-m molybdenum/lithium (Mo/Li) heat pipe was designed with an annular or screen tube wick. The design is shown schematically in Fig. 7. The screen tube fits inside the 19-mm-o.d., 1.5-mm-wall-thickness molybdenum container tube, with a 0.4-0.5 mm annular liquid return gap. This heat pipe contained a hafnium getter at the end of the evaporator in the form of loosely stacked foils. These were held in place on a molybdenum spool to facilitate assembly. The getter was intended to collect residual carbon, oxygen, and nitrogen from the lithium

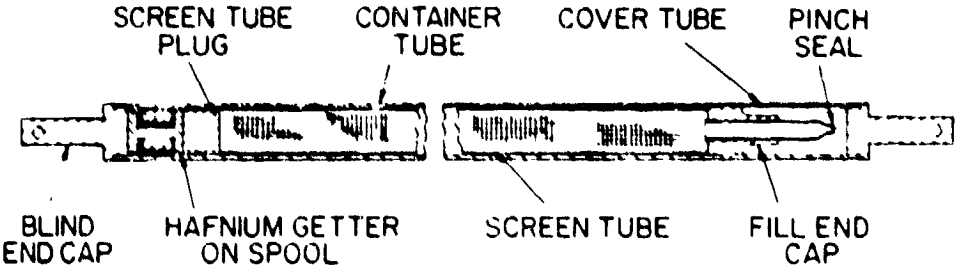

Fig. 7. Four-meter Mo/Li heat pipe.

The screen tube plug was also located in the evaporator end of the heat pipe. It was press-fit into the end of the screen tube in this heat pipe to seal the annulus so that the full capillary pumping force of the wick porosity could be obtained. The heat pipe was then sealed with a welded pinch seal enclosed in a cover tube. The latter served as a safety feature to prevent heat pipe failure due to leakage through the pinch seal during heat pipe operation. The performance goal for this heat pipe was an axial heat flux of 100 MW/m^2, or a total heat flux of 20 kW.

E. Fabrication.

Much of the development that went into establishing the fabrication procedures for this type of heat pipe has been detailed elsewhere[1], so only those procedures that were devised specifically for fabricating two 4-m Mo/Li heat pipes will be described in detail. The heat pipe fabrication was divided into three major operations: (1) screen tube production; (2) container tube procurement, processing, and assembly; and (3) heat pipe filling and sealing. These operations are detailed separately below.

1. Screen Tube. Two annular wicks were fabricated from 150 mesh molybdenum screen that was compressed between soft, low-carbon-steel tubes. These tubes were then removed by chemical dissolution and the compressed screen tube was sintered, forming a semirigid tube. The complete production sequence is diagrammed in Fig. 8. Most of the fabrication steps were carried out in facilities located at either the Oak Ridge National Laboratory (ORNL) or the Y-12 Plant, both in Oak Ridge, Tennessee, because they had available most of the equipment necessary to fabricate a long heat pipe.

The sheaths and mandrels between which the molybdenum screens were compressed began as commercially available, seamless, AISI 1018 steel tubes. The mandrel tube had a 19-mm outside diameter and a 3-mm-thick wall; the sheath had a 22.2-mm outside diameter and a 0.9-mm-thick wall. After all dirt, scale, and discolorations were mechanically removed, these tubes were hydrogen-annealed for 2 h at 1175 K to soften the metal. After annealing, these steel tubes were so crooked that the sheaths could not be easily slid over the molybdenum-screen-covered mandrels, so they were straightened in the roll straightener, seen in Fig. 9, before attaching the screen to the mandrel.

Before the screen was attached to the steel mandrel, it was cleaned in a warm water solution of a commercial product called Oakite 164 Aluminum Cleaner.

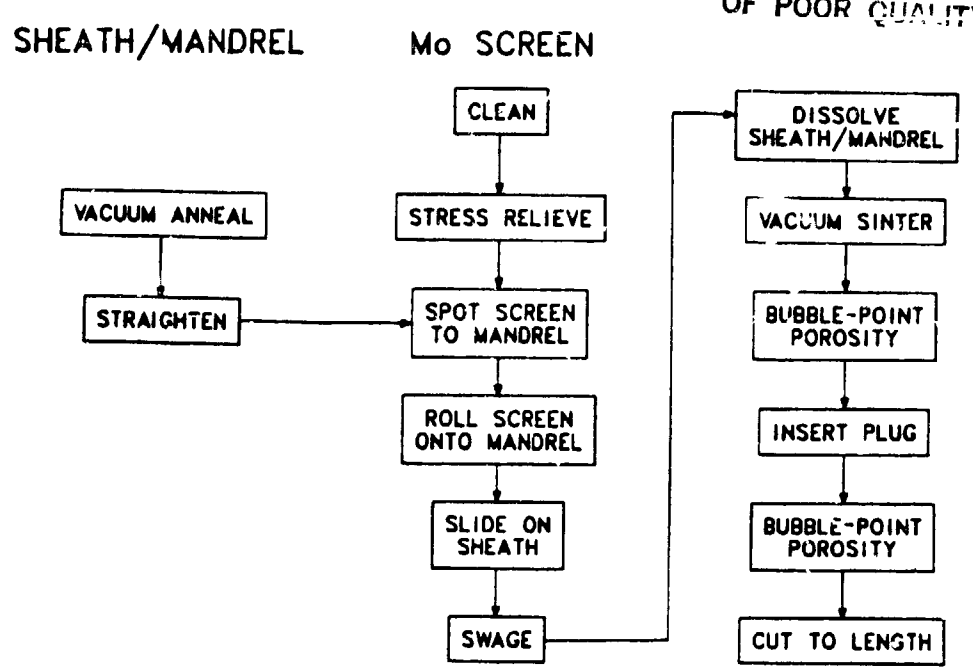

Fig. 8. Molybdenum screen tube wick fabrication flow diagram.

Fig. 9. Steel tube being straightened in roll straightener.

After rinsing and drying, the screen was stress relieved by vacuum annealing at 1125 K for 1 h. The cleaned and stress-relieved screen was then spot-welded directly to the mandrel, at intervals of 6 mm or less, with the spot welder shown in Fig. 10. Fairly sharp tungsten electrodes were used on the spot welder. One of the steel mandrels with the screen spot-welded to it can be seen in Fig. 11.

After the screen was spot-welded to the mandrel, it was hand-rolled onto the mandrel on a flat surface, as illustrated in Fig. 12. To allow the steel sheath to slide readily onto the coiled screen assembly, the screen was filled with ethanol just ahead of the sheath to act as a lubricant that could be easily removed during subsequent processing. As soon as the sheath was in place, the entire assembly was rotary swaged to the final size in two passes, starting with the four-jaw swage shown in Fig. 13. In the first pass, the sheath/mandrel assembly was

Fig. 10. Spot-welding molybdenum screen to a steel mandrel.

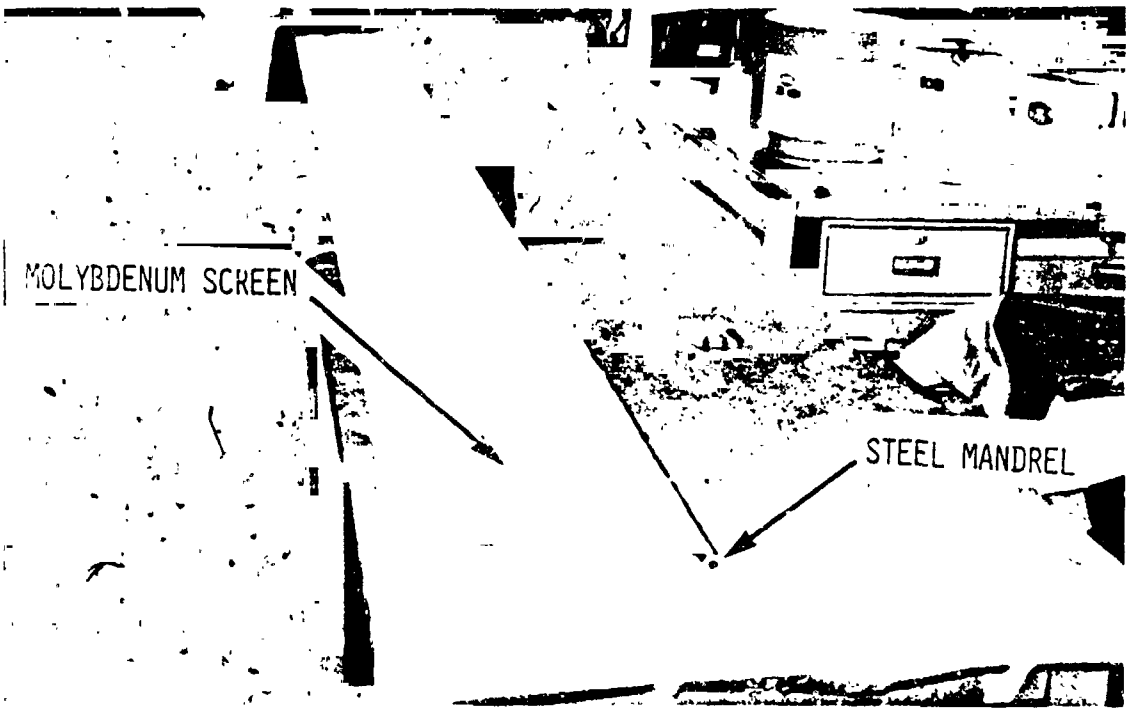

Fig. 11. Attachment of 305-mm-wide 150 mesh molybdenum screen to a 4.3-m-long steel mandrel by spot-welding.

Fig. 12. Molybdenum screen rolled on a steel mandrel, ready for insertion into the steel sheath.

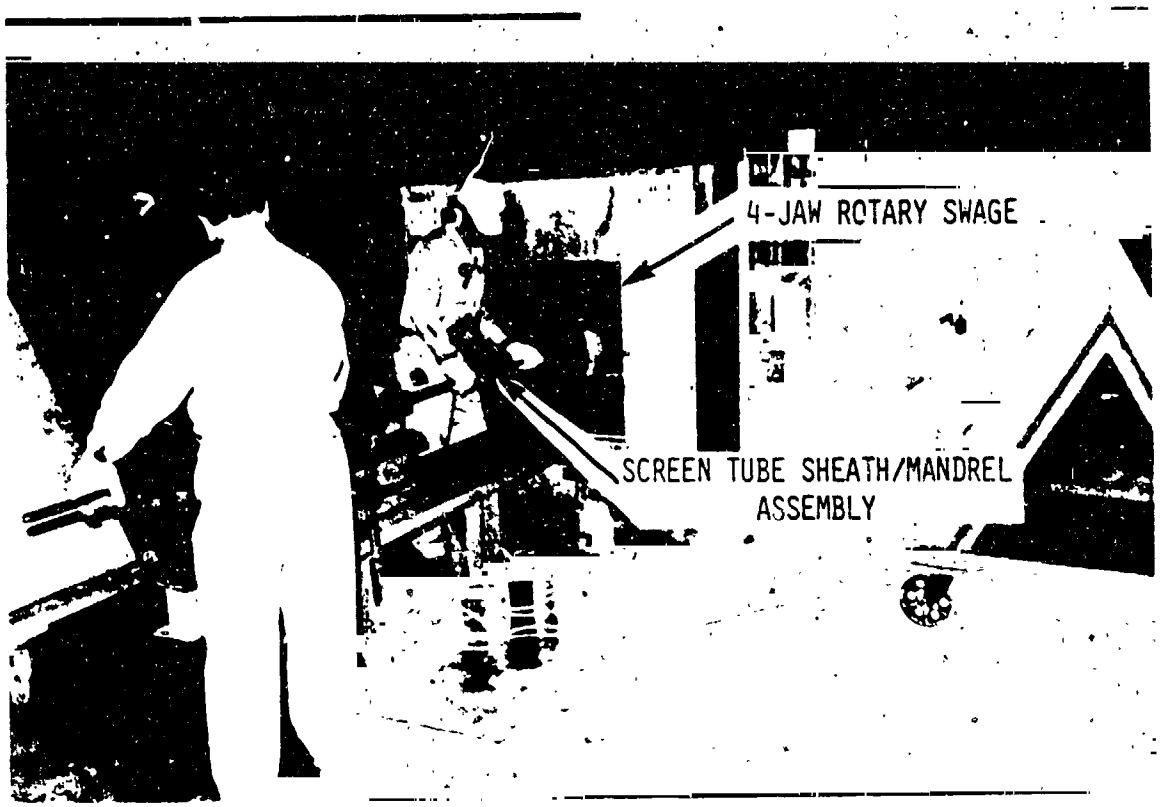

Fig. 13. Rotary swaging a molybdenum screen tube sheath/mandrel assembly.

run through an 18.3-mm-diam die set, and in the second pass, the assembly was run through a 17-mm-diam die set in a two-jaw rotary swage.

After swaging, the steel was dissolved away from the compressed molybdenum screen tube in a hot hydrochloric acid bath, which was contained in a long polyvinylchloride tray. The bath was heated by plastic steam lines submerged in it. The sheath was completely dissolved, but the mandrel was slid out of the screen tube after it was only partially dissolved. After the compressed screen tube was rinsed and dried, it was transported from ORNL to the Y-12 facility and placed in the 5.5-m-long radiant-heated, horizontal vacuum furnace shown in Fig. 14 for sintering. The compressed screen was bonded to form a semirigid tube by heating it for 2 h at 1725 K in a vacuum of 10^{-4} Pa or better.

The next step in the fabrication process involved bubble-point testing of the two sintered screen tubes to measure their effective porosity. This was accomplished by submerging the screen tube in 190 proof ethanol and pressurizing it internally with helium until the first bubbles formed. The pressure for bubble breakthrough is proportional to the largest pore in the screen tube. A photograph of the bubble-point test in progress on one of the finished molybdenum

Fig. 14. Five and one-half-meter-long tungsten mesh heating element vacuum furnace used for sintering and annealing.

screen tube wicks is shown in Fig. 15. One screen tube wick, which was designated MOST-7, had a bubble-point pore diameter of 44 μm; the other screen tube, MOST-8, had a pore diameter of 60 μm. The outside diameter of MOST-7 ranged from 14.96 to 15.09 mm, and its wall thickness was 165 μm. The outside diameter of MOST-8 ranged from 15.14 to 15.24 mm, and its wall was 178 μm thick.

As can be seen in the scanning electron micrographs in Fig. 16, the wires in the finished screen tube are highly deformed and nested. The wires were sufficiently bonded together to allow the screen tube to be handled without fear of unwinding it. Chemical analyses of the MOST-7 screen tube indicated that it contained 260 ppm oxygen, 170 ppm carbon, 15 ppm nitrogen, and 760 ppm iron in the finished condition.

After the porosity of the screen tubes was determined, a tapered molybdenum plug was press-fit inside one end of the heat pipe. The bubble-point porosity test was then repeated to make sure that the fit of the plug was tight enough so that the equivalent pore diameter of the interface between the plug screen was

Fig. 15. Bubble-point porosity measurement being performed on a molybdenum screen tube wick

no larger than that of the screen tube itself. When the plug was determined to be tightly installed, the screen tube was ready for insertion into the heat pipe container tube.

2. Container. Two 4-m-long, 19-mm-o.d., 1.5-mm-thick wall low-carbon arc-cast (LCAC) molybdenum seamless container tubes were produced by the Metals Division of ThermoElectron Corporation. The tubes were produced by drawing gun-drilled tube blanks through dies over fixed mandrels at about 480 K. Both finished tubes were sent to AMAX Specialty Metals in Cleveland, Ohio, where they were cleaned with a molten caustic containing about 10% sodium nitrite. After

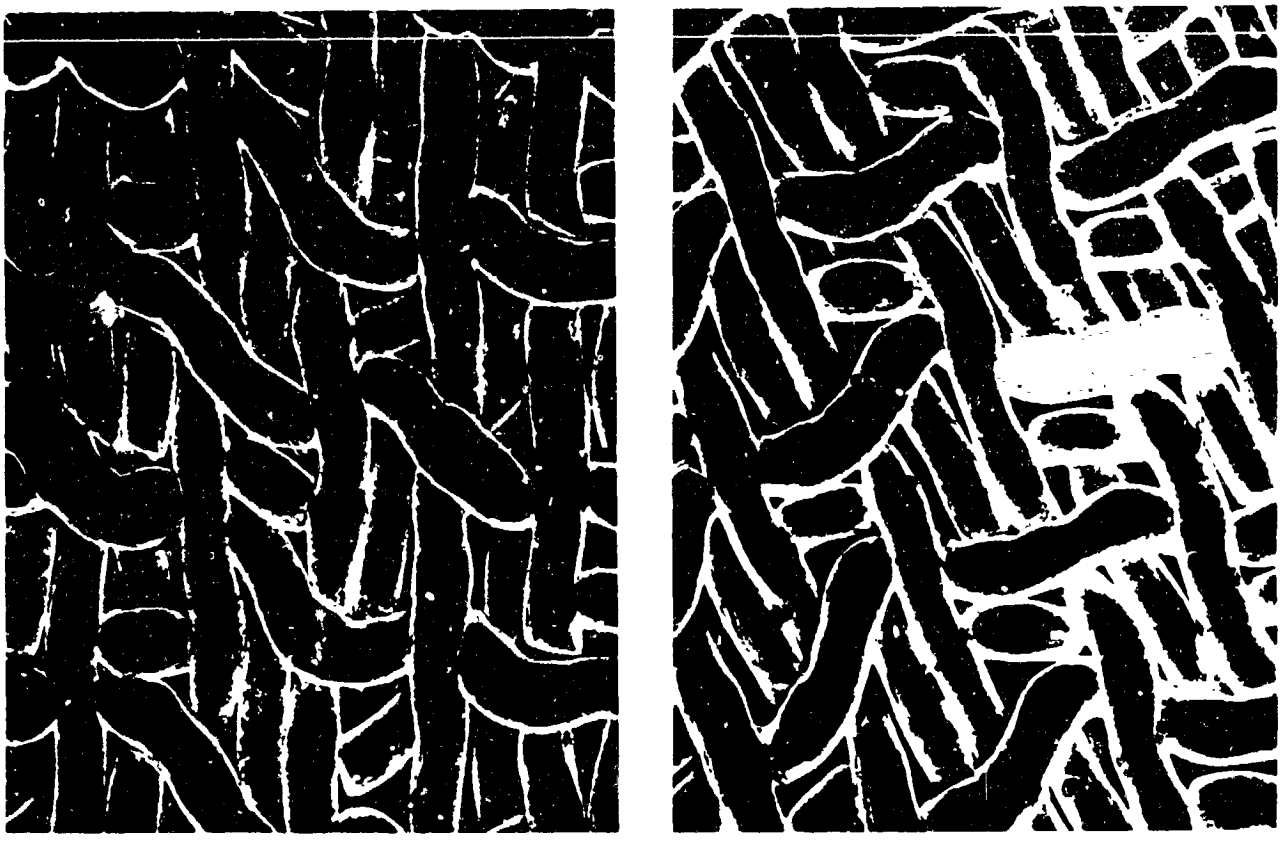

a. Inside (140 X). b. Outside (140 X).

Fig. 16. Scanning electron micrographs of (a) the inside surface and (b) the outside surface of the finished molybdenum screen tube MOST-7.

cleaning, the container tubes were vacuum annealed in the Y-12 vacuum furnace (Fig. 14) for 2 h at 1725 K. The impurity analysis of the molybdenum tubes at this point indicated they contained 30 ppm carbon, 6 ppm oxygen, less than 1 ppm nitrogen, and 10 ppm iron.

As shown in Fig. 17, the inside surface of the container tube was fairly rough on a microscopic scale. The internal microstructure of the tube material after the vacuum anneal is shown in Fig. 18. The metal can be seen to be completely recrystallized and to contain a few uniformly distributed precipitates that are probably carbides. A measurement of the hardness of this material gave a value of 190 DPH, which was comparable to similar molybdenum tubing that had no precipitates. This tubing tended to be significantly more ductile at room temperature than previously examined molybdenum tubing in that it could be given at least one cycle of 90° reverse bends before failure. As can be seen in the

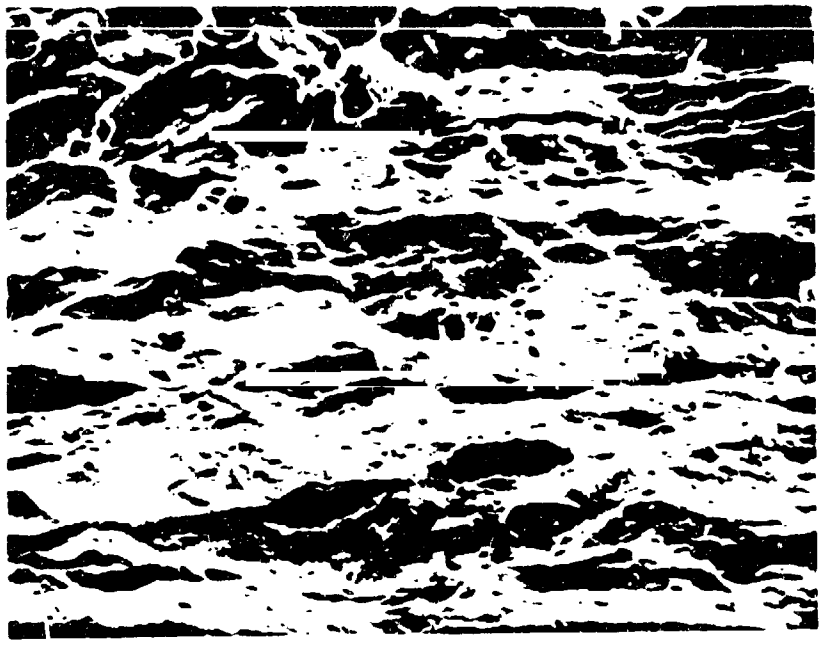

Fig. 17. Scanning electron micrograph of the inside surface of the NEP-1A molybdenum container tube. (750 X)

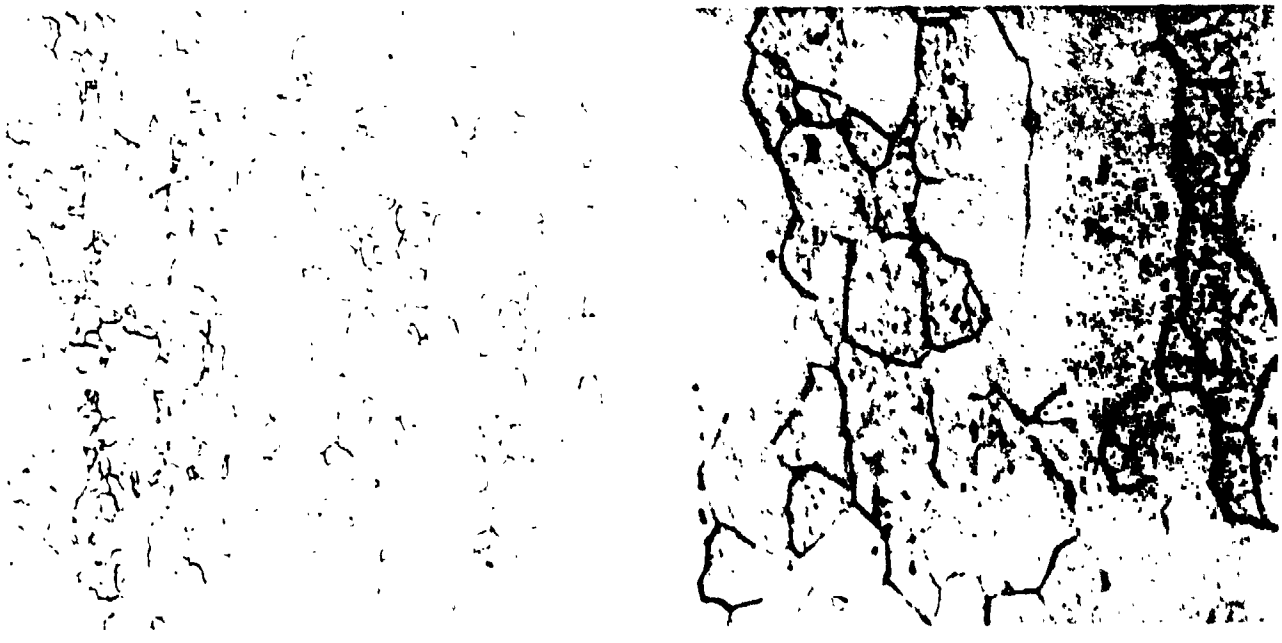

a. 100 X. b. 500 X.

Fig. 18. Microstructure of the NEP-1A molybdenum container tube after vacuum annealing 2 h at 1725 K.

fractograph in Fig. 19, the failure was mostly transgranular, which differs significantly from other molybdenum tubing we have studied that typically fails in a mostly intergranular fashion.

All the end caps shown in Fig. 7 were machined from molybdenum bar stock and electron beam (EB) welded into the container tube at the Oak Ridge Y-12 plant. Before joining the fill end cap to the heat pipe, a 6.4-mm-o.d., 0.8-mm-wall molybdenum fill tube was EB welded to it. This fill tube had previously had a stainless steel Swagelok fitting vacuum-brazed to it using copper as the filler metal. This was to allow for later attachment of the heat pipe to a stainless steel pot, from which the lithium would be distilled. After the blind end cap was welded in place and found to be helium leak-tight, the screen tube was inserted and the fill end cap with its attachments was welded in place.

3. Heat Pipe Reassembly. After the two heat pipes were assembled at Oak Ridge, they were shipped to Los Alamos for filling. The heat pipes were carefully packaged individually inside electrical-mechanical tubing, then well packed inside a single aluminum tube, and finally, shipped to Los Alamos by air freight. Somewhere in transit the package was dropped a considerable distance,

Fig. 19. Scanning electron micrograph of the fracture surface of the NEP-1A molybdenum container tube in the vacuum annealed condition.

and the contents were broken. When the package was received and opened, the fill tubes were found to be broken off both of the heat pipes, as shown in Fig. 20(a) and, as can be seen in Fig. 20(b), one of the container tubes was broken in two. When the screen tube wicks were removed from the molybdenum container tubes, it was found that both wicks had also been broken in several locations [Fig. 20(c)].

The pattern of the breakage was such that it was possible to salvage an undamaged section of screen tube wick about 2 m long from each of the broken heat pipes. These two sections were connected together with a tapered, tubular molybdenum coupler that was press-fit inside the bore of the screen tubes. This reduced the bore of the heat pipe near its center to 13 mm for a distance of about 25 mm. No leaks were observed in the final assembly at either the coupler or the refitted screen tube plug, and the bubble-point pore diameter of the final assembly was to be 44 μm. This assembly was inserted in one of the container tubes that had been reassembled and cut to the length of the new two-piece screen tube. The entire reassembly, which was performed at Los Alamos, required assembly of an extension to the vacuum chamber of our EB welder long enough to enclose the entire heat pipe.

4. Filling. Filling of the heat pipe with lithium was first attempted using the procedures developed for sodium and described in Ref. 1. This process involved distilling the lithium through the copper-brazed stainless steel/molybdenum tube joint that was required to connect the stainless steel fill pot to the molybdenum heat pipe. Because of the high distillation temperature for lithium, above 1025 K, and the high solubility of copper in lithium, the joint developed a leak during the distillation process, and most of the lithium was lost into the vacuum chamber. Distillation of the lithium into the heat pipe was attempted at 1050 K, a temperature later determined to be too low to prevent blockage of the fill tube with liquid lithium. The blockage of the fill tube resulted from the fact that the vapor pressure of lithium was not sufficient to overcome the surface tension forces in the fill tube.

A second attempt at filling the 4-m heat pipe involved distilling the lithium into a chamber whose volume was set to equal that required to fill the heat pipe to the desired level. The lithium was then transferred as a liquid to the heat pipe through a stainless steel tube. A schematic diagram of the apparatus is presented in Fig. 21. The stainless steel distillation chamber contained

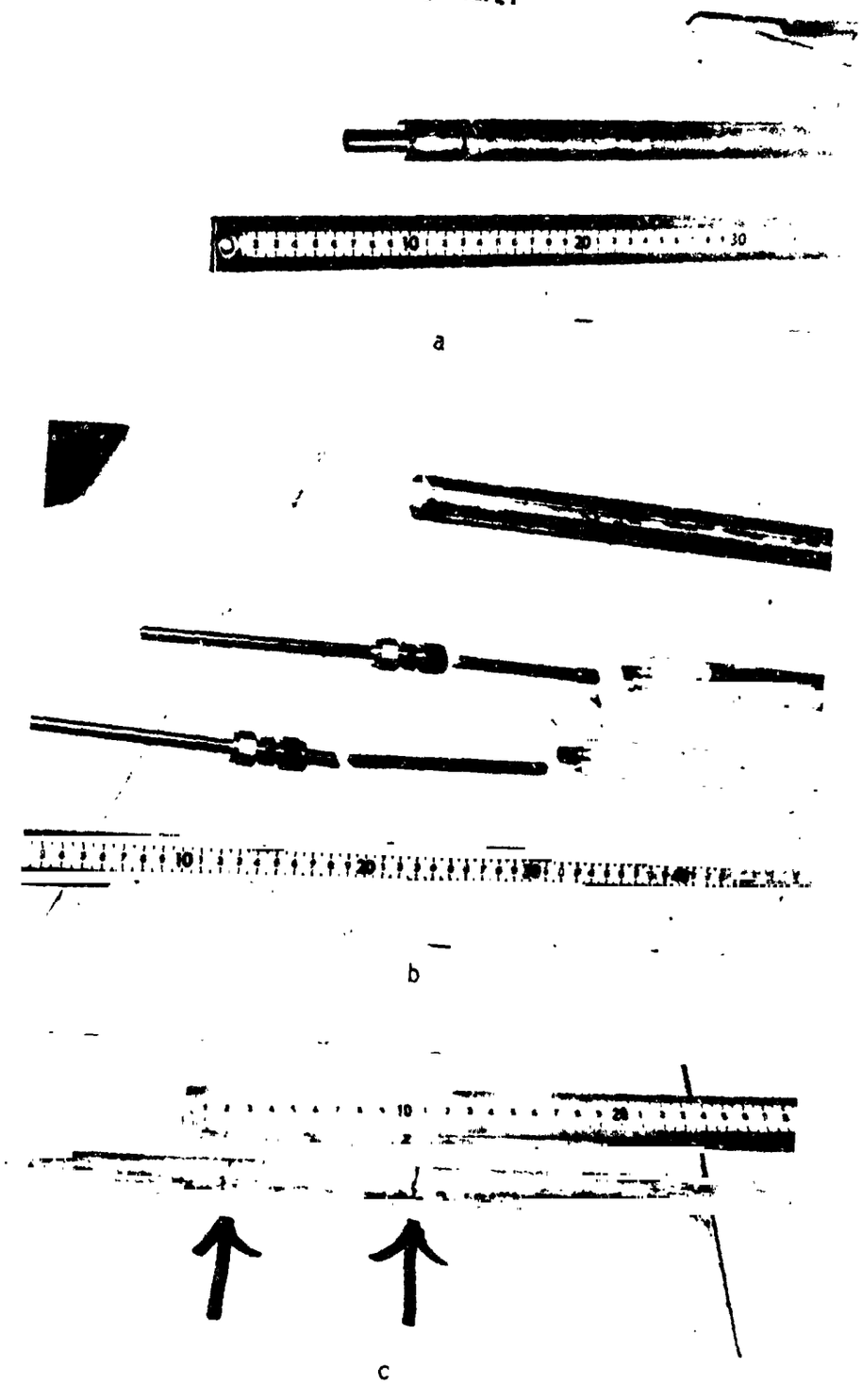

Fig. 20. Fractured (a) fill tubes, (b) container tubes, and (c) screen tube from 4-m NEP heat pipes damaged in shipment.

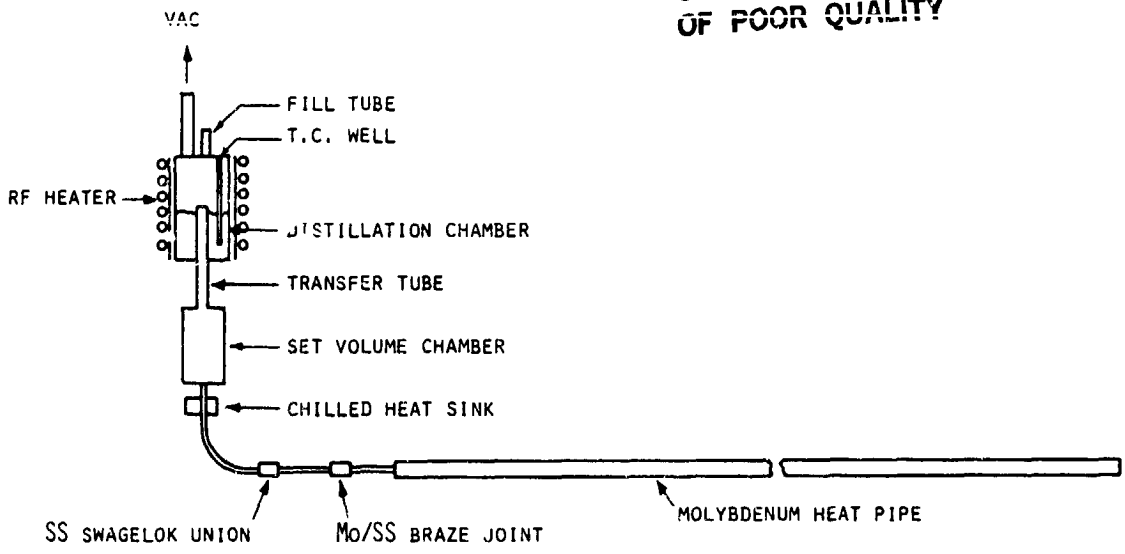

Fig. 21. Heat pipe distillation chamber.

multiwrapped, 100 mesh stainless steel screen, which prevented liquid slugging during the distillation process.

The distillation chamber was heated by rf induction. The set-volume chamber was attached to the distillation chamber by a stainless steel tube extending through the lithium pool. The combined volume of the transfer tube and the chamber was 140 cm^3, the amount needed to fill the heat pipe. A secondary transfer tube made with standard-wall 0.25-in.-diam stainless steel joined the bottom of the set volume chamber to the heat pipe. The chilled heat sink was placed just below the chamber to act as a valve to prevent lithium from draining out of the chamber during distillation.

The total operation of transferring lithium from the distillation chamber to the heat pipe was done as follows. The entire system was evacuated, and the lithium pool was heated and degassed. When the lithium temperature reached 1000 K, the vacuum system was closed off. The lithium temperature was then increased to 1200 K, where distillation began. The distillation was complete when the volume from the heat sink to the top of the transfer tube was filled with lithium.

The distillation chamber was cooled to 600 K and the heat sink was removed. The heat pipe, the 0.25-in.-diam transfer lines, and the set-volume chamber were then heated to 500 K, allowing the liquid lithium to drain by gravity into the heat pipe.

After fill and pinch seal closure, a protective end cap was EB welded over the pinch seal to complete the filling operation.

C. Testing.

The heat pipe was placed in a 5-m-long quartz tube and heated in vacuum with a 1-m-long rf heat-input coil. The first operation was to slowly heat the heat pipe in the horizontal position to allow lithium fluid to completely wet the annular screen structure. The temperature was gradually increased until a distinct hot spot appeared prematurely in the evaporator section near the end of the heat pipe.

Such a hot spot indicates a dryout condition, caused by improper wetting of the interior surfaces of the heat pipe by lithium. This occurrence was thought to be caused by an excess of oxygen in the heat pipe screen structure. Removal of this oxygen required that it be transported to the gettering material located in the evaporator at the very end of the heat pipe, outside of the heated zone. Because the heat pipe would not operate at high enough temperatures (>1100 K) to getter the oxygen from the condenser end all the way to the evaporator, a small heating coil was positioned at the condenser end of the pipe. This coil was gradually moved, in steps, toward the evaporator end of the heat pipe. It was expected that oxygen in the pipe in the vicinity of the coil would be deposited in the center of the heated zone and, as the heated zone was moved toward the evaporator, all the oxygen in the pipe would be transferred to the evaporator end of the pipe. This step procedure was carried out until the coil was at the location of the gettering material in the evaporator end of the heat pipe. Although this operation resulted in a distinct improvement in heat pipe performance and higher overall temperatures in the evaporator were achieved, the hot spot still occurred, limiting the heat input into the heat pipe.

Rather than repeat the time-consuming procedure outlined above to transport the remaining oxygen to the evaporator, a different mode of operation was set up to accomplish the same task. An attempt was made to raise the operating temperature of the whole pipe by using two heating coils. One, the driver coil, about 30 cm long, was located at the evaporator end of the pipe, and a second, low-power coil was wrapped around the remaining length of the pipe. By this method it was possible to raise the temperature of the entire heat pipe to 1300 K while maintaining the hot spot temperature in the evaporator where the oxygen was collecting below 1700 K. After a few hours of operation, and without any change in power to the second coil, it was possible, by increasing power to the driver

coil, to raise the heat pipe temperature to 1400 K and still not exceed a hot spot temperature of 1700 K. This observation indicates that oxygen was indeed slowly being removed from the pipe to the gettering material. It was not possible, however, to operate the pipe without the secondary coil and, consequently, it was not possible to estimate the power transferred by the pipe.

The pipe was subsequently operated in several tilted positions, with the evaporator elevated above the condenser. The heat pipe was operated at 1325 K for a period of 3 h, then shut off. The evaporator end was raised in increments of 100 mm, and the heat pipe restarted at 1325 K and held for 3 h. This procedure was repeated until an elevation of 1 m was reached, at which point the pipe failed to restart without exceeding the hot spot temperature of 1700 K. Ideally, the pipe should have been able to operate in the fully vertical position because the wick pore size was fine enough to wick lithium up a height of 4 m. Repeated efforts to clean the pipe of oxygen contamination by operating in the horizontal position for 2-3 h, then elevating the evaporator end to 1 m, did not show any improvement in heat pipe performance, so testing of the pipe was terminated.

Renewed testing of this heat pipe will involve extensive effort in several areas. First, the pipe will have to be opened to remove the screen wick for inspection. Assuming the wick to be in satisfactory condition, it will be necessary to perform a new porosity test. A facility to clean and degas a 4-m-long heat pipe in vacuum and at high temperature will have to be built. The heat pipe would then be refilled using the latest technique of continuous pumping, with a getter material located in the distillation pot. The pipe could be tested again relatively easily in a quartz system, but with the use of thermal radiation shields instead of a secondary rf coil to bring the pipe up to operating temperature. This arrangement would permit measuring the power transferred by the pipe by a determination of the radiation losses. However, more extensive testing would require construction of a test chamber with calorimeter, large enough to hold a 4-m heat pipe.

V. DISCUSSION

It is clear from the shielding studies that reducing the allowable gamma exposure at 25 m from 10^7 to 10^6 in 7 yr has a more adverse effect on shield weight than an order-of-magnitude reduction of allowable neutron fluence to 10^{12} nvt. Thus it would pay more, in terms of payload delivered to the outer

planets, to harden the science package to gammas as opposed to neutrons. Because the weight penalty for the extra shielding is quite substantial, it would be worthwhile, in addition to hardening investigations, to examine whether radiation-sensitive experiments can be done during times of reduced reactor power.

The Monte Carlo calculation of the effect of water immersion on reactor reactivity indicates that the judicious location of a modest amount of B_4C will guarantee subcriticality for the immersed reactor. More detailed design work must be done to establish the most appropriate configuration for the B_4C, with simplified removal methods once a safe orbit is reached--an important design consideration.

Although the work on the 4-m heat pipe did not produce a unit operating with the desired performance, it did show that the fabrication and installation procedures for long wicks are relatively straightforward extensions of procedures established for shorter lengths. It also showed that survival of shuttle launch is not the only reason to be concerned about the brittleness of recrystallized molybdenum at room temperatures. Even terrestrial transport requires extraordinary packaging methods. This experience has led to a shift to Mo-14 Re alloy as the baseline material for reactor core heat pipes. The latter material is still in the developmental stage, but has been shown to have a ductile-to-brittle transition temperature below 200 K. Even EB welds in this alloy maintain ductility at this temperature.

The observation of hot spots in the heat input zone indicated the presence of lithium oxide in the heat pipe. Efforts to keep the levels of oxygen in the heat pipe wick and wall materials to very low levels through all the processing steps have been redoubled. It is believed that the primary source of oxygen in the heat pipe, however, is from the lithium itself and that the distillation filling procedure is not removing it completely. This has led to the ordering of ultrahigh purity lithium from ORNL. All future core heat pipes will use this material.

REFERENCE

1. L. B. Lundberg and H. E. Martinez, "Fabrication of High-Temperature (1400-1700 K) Molybdenum Heat Pipes," in Proc. of the 15th IECEC, August 18-22, 1980, Seattle, WA.